The Control and Characterization of the Crystallographic Texture of Longitudinal Thin Film Recording Media

David E. Laughlin, Li-Lien Lee, Li Tang and David N. Lambeth
Date Storage Systems Center, Carnegie Mellon University, Pittsburgh, PA 15213

***Abstract*—In this overview we summarize our methods of changing important microstructural features such as grain size and crystallographic texture, in magnetic thin films for longitudinal recording. The methods we have used to better control the grain size and texture of the magnetic films include the use of different *underlayers* (NiAl and FeAl), the use of *seed layers* underneath the underlayers and the use of *intermediate layers* between the underlayer and the magnetic thin film. Examples of the structure and magnetic properties of such films will be presented and discussed. We also present our newly developed method of quantitatively characterizing the crystallographic textures of the thin films used in the multilayered structures. Our method relies on the examination of the intensity weighted reciprocal lattice by means of tilted electron beam diffraction patterns. These patterns contain arcs, the number and location of which can be correlated with specific thin film textures. We will present an overview of the technique from the point of view of the reciprocal lattice and include an example which shows how the crystallographic texture of thin films can be examined and characterized.**

INTRODUCTION

In order to improve the magnetic properties of thin film longitudinal magnetic recording media, it is necessary to better control the microstructure of the magnetic layer. An example of this comes from work of the 1980's when BCC Cr was introduced as an underlayer for HCP Co-based thin films for magnetic recording. It was observed that this increased the in-plane coercivity of the Co-based films. When the Cr was deposited on a heated substrate the coercivity increased even more. It was determined that the heated substrate induced Cr underlayer with a (002) crystallographic texture. Earlier single crystal work [1] had shown that the $(11\bar{2}0)$ planes of Co-based film epitaxially grew on the (002) planes of Cr. Thus, by controlling the crystallographic texture of the underlayer, the texture of the magnetic film could be changed which in turn changed the magnetic properties of the Co-based film. This is a good example of the basic paradigm of Materials Science, namely that the extrinsic properties of a material (in this case the coercivity) depend on its structure (crystallographic texture), which in turn can be controlled by changing certain processing conditions (the temperature of the substrate).

Over the past several years we have been controlling the magnetic microstructure of thin film media by varying the microstructure of the underlayer [2, 3] by means other than by changing the process variables. Herein we will summarize our methods of changing the important microstructure features, such as grain size and crystallographic texture, and we will also present our newly developed method of characterizing the crystallographic texture of the thin films.

For fixed sputtering conditions, the microstructural features of the magnetic layer such as elemental segregation, grain size and crystallographic texture can be strongly affected by structural features below it (the underlayer and the substrate) but only slightly affected by its overlayer. We have utilized several changes to the standard configuration of longitudinal thin film media trying to modify the magnetic layer/underlayer and underlayer/substrate interfaces. Our terminology for the different layers is shown in Fig. 1. We have named the layers in reference either to their positions with respect to the magnetic layer (the underlayer lies *under* the magnetic layer and the intermediate layer lies *between* the underlayer and the magnetic layer) or with a name that describes its function (the seedlayer *seeds* the nucleation of a particular crystallographic texture of the underlayer).

NEW UNDERLAYERS

One way of changing the microstructure of the underlayer is to change the material of which it is made. We have looked at several ordered intermediate phases with the B2 structure, which is closely related to the BCC Cr structure. We also have utilized sputtered MgO as an underlayer.

The intermetallic compound NiAl has the B2 crystal structure (space group $Pm\bar{3}m$; prototype CsCl). Since its lattice parameter is nearly the same as that of BCC Cr, the

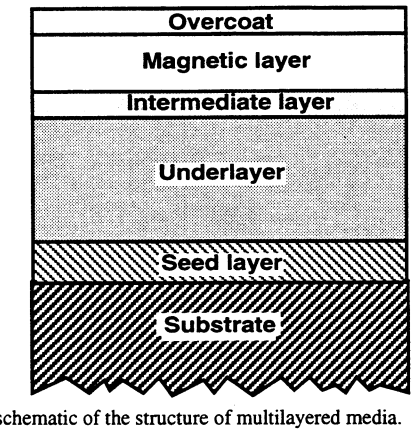

Fig. 1. A schematic of the structure of multilayered media.

0018-9464/96$05.00 © 1996 IEEE

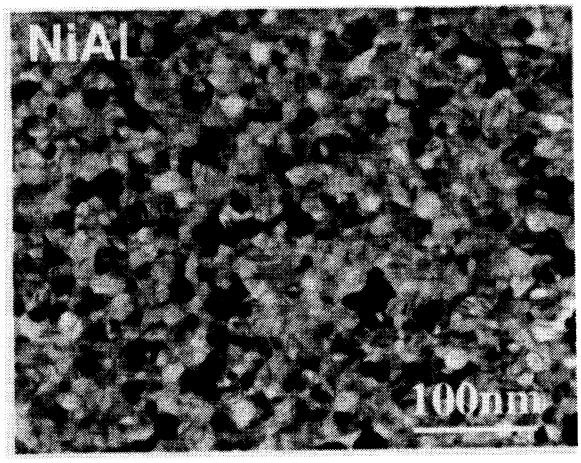

Fig. 2. Bright field TEM micrograph of a RF sputtered 100 nm NiAl film on glass. The grain size is ~15 nm.

various epitaxial relations that occur between Co-based alloys and Cr should also occur between Co-based alloys and NiAl [4]. We have sputter deposited NiAl on glass substrates and have obtained films with grain sizes that are approximately 15 nm (Fig. 2) which are about half of the diameter of comparably sputtered Cr films. The signal to noise ratio of media produced on such underlayers is improved, probably due to the smaller and more uniform grains [5]. The coercivity values are about the same as those deposited on Cr underlayers.

We have also used FeAl as an underlayer. We obtained similar results as with NiAl [6].

MgO (B1 structure, space group Fm $\bar{3}$m, prototype NaCl) has also been used as an underlayer. Figure 3 shows a schematic of its B1 structure. When sputtered at room temperature we obtained films with the (002) texture. This enables the Co-based alloy to form with its c-axis in the plane of the film, because of the epitaxial relationship. Also of

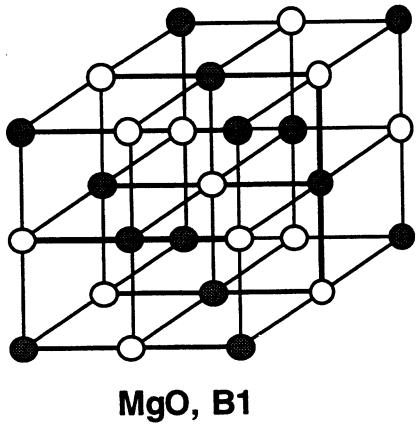

Fig. 3. Crystal structure of MgO.

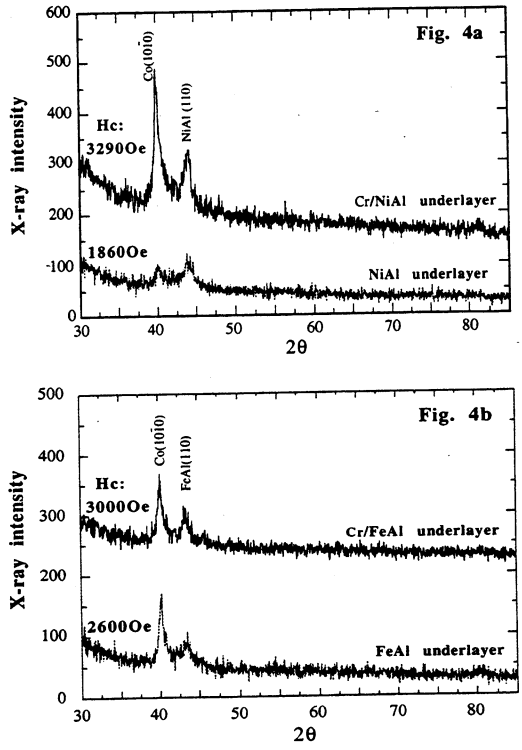

Fig. 4. X-ray diffraction spectra of 40 nm CoCrPt on (a) 100 nm NiAl underlayers with and without a 2.5 nm Cr intermediate layer (b) 100 nm FeAl underlayers with and without a 2.5 nm Cr intermediate layer.

interest is to note that this would give rise to an in-plane c-axis (11$\bar{2}$0) type Co texture without using high temperature sputtering.

Thus, by using a different underlayer, microstructural features such as grain size and crystallographic texture can be controlled and this in turn can improve the magnetic properties of the Co based media.

INTERMEDIATE LAYERS

The amount of interdiffusion and epitaxy between the magnetic layer and the underlayer can be further changed by inserting a thin intermediate layer at their interface. If the intermediate layer has an atomic structure similar to either the HCP magnetic layer or the BCC/B2 underlayer the change in grain size and epitaxial effects of the underlayer will be small.

The addition of a 2.5 nm thick Cr *intermediate* layer to the above mentioned new underlayers greatly enhances the coercivities of the subsequently deposited CoCrPt films without compromising the (10$\bar{1}$0) CoCrPt texture. See Fig. 4 for two examples. Another kind of *intermediate* layer has been developed by Fang and Lambeth [7]. They sputter deposited a thin layer of CoCrTa between a Cr underlayer and a CoCrPt thin film. This improved the lattice matching of the

CoCrPt film and thereby improved the in plane magnetic properties of the CoCrPt film. This layer of CoCrTa acts like the Cr intermediate layer on the NiAl underlayer. It has the same structure as the magnetic film, while the Cr *intermediate* layer has a similar structure to the underlayer. Since both are in between the underlayer and the magnetic layer we call them *intermediate* layers.

MgO SEED LAYERS

The work of Nakamura *et al.* [8] suggested to us that MgO might be a suitable underlayer. They demonstrated that Cr films deposited on single crystals of (002) MgO have a (002) crystallographic texture. This occurs because of epitaxial atomic matching across the interface as illustrated in Fig. 5. Building on this concept we believed that MgO would be a good *seed layer* for subsequently deposited underlayers. By sputtering MgO onto glass substrates we obtained polycrystalline MgO films with strong (002) crystallographic textures [9]. This texture is expected since MgO has the B1 crystal structure which has its {002} planes as the ones with the lowest surface energy [10]. This strong (002) textured MgO then can act as a seed layer for the growth of a highly textured Cr underlayer (or NiAl underlayer). Of interest here is that the (002) Cr crystallographic texture can be obtained without preheating of the substrate. Fig. 6 shows the x-ray diffraction patterns for films produced with and without the (002) textured MgO seed layer, along with the resulting in-plane coercivities. The (002) textured MgO seedlayer is seen to change the texture of the Cr underlayer from (110) to (002), which in turn changes the texture of the CoCrPt alloy magnetic layer from (0002) to $(11\bar{2}0)$.

NiAl layers also grow with the (002) texture on the (002) textured MgO seed layers. However, in contrast to the (002) Cr on the (002) MgO seed layer which induces the $(11\bar{2}0)$ texture of the CoCrPt magnetic layer, the grain to grain epitaxial relationship between the (002) NiAl and the CoCrPt film is found to be $[10\bar{1}1]$ CoCrPt//[001] NiAl, and $(1\bar{2}10)$ CoCrPt//(100) NiAl (variant 1), or $(1\bar{2}10)$CoCrPt//(010) NiAl (variant 2) [11].

ELECTRON DIFFRACTION STUDY OF THIN FILM TEXTURE

As indicated above, the crystallographic texture of the thin magnetic film is of great importance in the determination of its extrinsic magnetic properties. It is sometimes possible to obtain qualitative information about the texture of the magnetic thin films from standard $\theta/2\theta$ X-ray scans. See for example Figure 6 above. However, sometimes the X-ray scan does not give a clear indication of the crystallographic texture of the thin film, either because the film is too thin for good diffraction, or possibly because the texture is such that a set of low index planes is not parallel to the plane of the film [11].

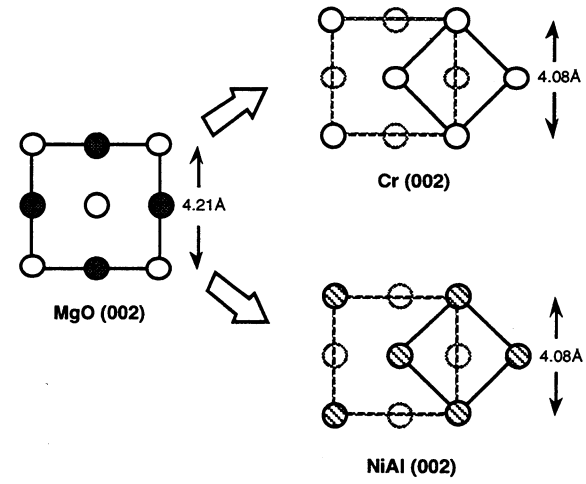

Fig. 5. Atomic matchings of MgO (002) to Cr (002) and NiAl (002).

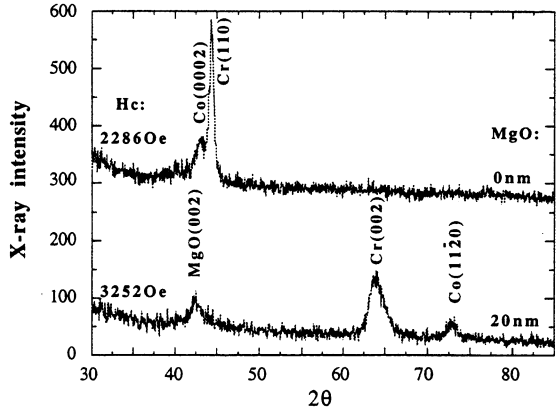

Fig. 6. X-ray diffraction spectra of CoCrPt(40 nm)/Cr(100 nm) films with and without a 20 nm MgO seed layer.

We have developed a technique to study the texture of thin films in the transmission electron diffraction mode [12, 13]. Our approach is different from the previous work [14, 15] in that we treat fibrous and lamellar texture in a unified way. Here we will summarize it briefly and give an example of its use.

For fibrous and lamellar textured thin films, the reciprocal lattice of an {hkl} family of planes consists of reciprocal circles around the texture axis. The number of the reciprocal circles is the number of distinct angles between the {hkl} planes and the texture axis. If the texture axis has an angular distribution α the reciprocal circles became reciprocal spherical belts with an angular width of 2α from the origin of the reciprocal lattice. Fig. 7 shows schematically the intersection of the Ewald sphere (which can be approximated as a plane for high energy electrons since the radius of the Ewald sphere is proportional to the reciprocal of the wavelength of the electron beam) with the reciprocal lattice of an {hkl} family of planes (belts of -hkl$_1$ and -hkl$_2$ are not shown here for clarity). In this case the {hkl} planes make

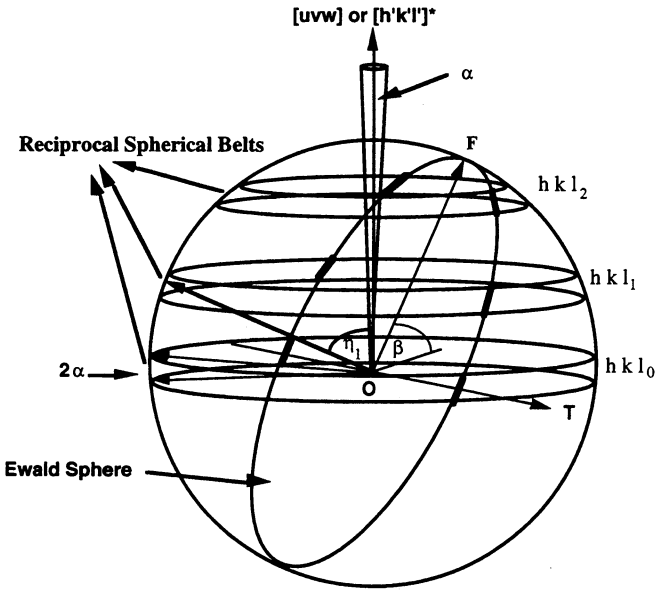

Fig. 7. Interaction of Ewald sphere with the reciprocal lattice of a textured film.

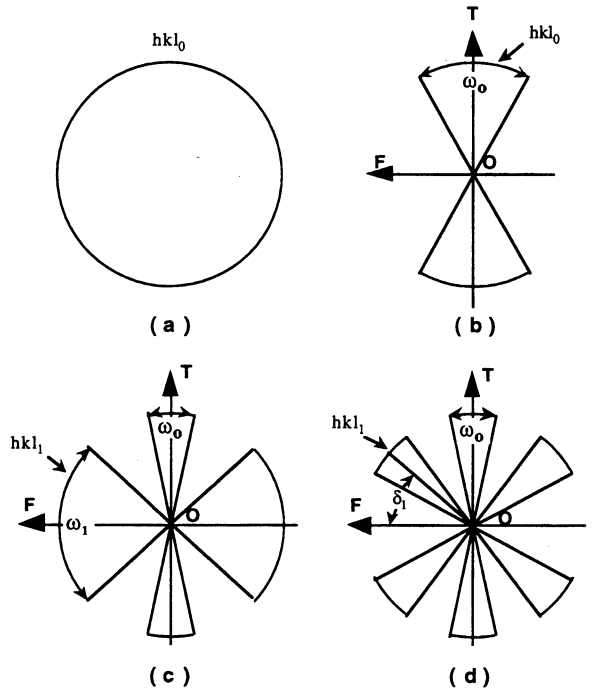

Fig. 8. Diffraction pattern evolution with tilt angle of an {hkl} family of planes having two distinct angles (one is 90°) with the texture axis (a) 0° tilt, (b) $\alpha < \beta < \beta_1^s$, (c) $\beta_1^s \le \beta \le \beta_1^e$ and (d) $\beta_1^e < \beta \le 90°$ (β: tilt angle).

three distinct angles (one of them is 90°) with the texture axis ([uvw] for the fibrous texture and [h'k'l']* for the lamellar texture). In Fig.7:

OT is the tilt axis in the film plane,

OF is the direction perpendicular to both the **OT** and the incident electron beam direction,

β is the angle between the Ewald sphere and the reciprocal plane which the texture axis is normal to,

η_i, i = 0, 1, 2 are angles between the reciprocal circles hkl_0, hkl_1 and hkl_2 and the texture axis.

Fig. 8 shows the evolution of the electron diffraction patterns as the tilt angle β increases. The diffraction pattern shown here arises from an {hkl} family of planes having two distinct angles (one is 90°) with the texture axis. It can be noted that the hkl_0 ring at $\beta = 0$ (Fig. 8a) breaks into two arcs, which bisect the **OT** axis and are symmetric about the origin with an angular width of ω_0, when $\beta > \alpha$ (Fig. 8c-d). It can also be seen that ω_0 decreases as β increases. Besides the hkl_0 arcs, hkl_1 and $-hkl_1$ arcs bisecting the **OF** direction and being symmetric about the origin appear when $\beta = \beta_i^s$ where $\beta_i^s = 90° - \eta_1 - \alpha$ (Fig. 8c). The angular width ω_1 subtended by the hkl_1 arcs increases with increasing β. Each of the hkl_1 arcs splits into two arcs with an angle of δ_1 from the **OF** direction when $\beta > \beta_1^e$, where $\beta_i^e = 90° - \eta_1 + \alpha$ (Fig. 8d). In general, it can be proved that the following relations hold [12, 13]:

$$\sin(\omega_0/2) = \sin(\alpha) / \sin(\beta) \qquad \alpha \le \beta \le 90° \qquad (1),$$

$$\cos(\omega_{hkli}/2) = \sin(\beta_i^s) / \sin(\beta),$$
$$i = 1, 2,...N, \text{ or } N-1 \quad \beta_i^s \le \beta \le \beta_i^e \qquad (2),$$

$$\sin(\omega_0/2) = \sin(\alpha) \cos(\omega_{hkli}/2) / \sin(\beta_i^s),$$
$$i = 1, 2, ...N, \text{ or } N-1 \quad \beta_i^s \le \beta \le \beta_i^e \qquad (3),$$

$$\cos(\eta_i) = \sin(\beta) \cos(\delta_i),$$
$$i = 1, 2,...N \text{ or } N-1 \quad \beta_i^e < \beta \le 90° \qquad (4),$$

$$\beta_i^s = 90° - \eta_i - \alpha, \quad \text{and}$$
$$\beta_i^e = 90° - \eta_i + \alpha, \quad i = 1, 2,...N, \text{ or } N-1 \qquad (5).$$

where N is number of distinct angles of {hkl} family of planes with the texture axis.

Thus, the texture axis direction indices can be determined by using Eq. (4) with the known tilt angle β and measured δ_i values. Meanwhile, the texture axis distribution angle α can be determined from the slopes of the straight lines of $\sin(\omega_0/2)$ vs. $1/\sin(\beta)$, $\cos(\omega_{hkli}/2)$ vs. $1/\sin(\beta)$, and $\sin(\omega_0/2)$ vs. $\cos(\omega_{hkli}/2)$ plots.

The patterns shown in Figure 9 are electron diffraction patterns at different tilt angle from a [001] textured Cr film which is often used as an underlayer for magnetic recording films in rigid disks. The diffraction patterns due to {110} planes is consistent with that shown in Figure 8 since {110}

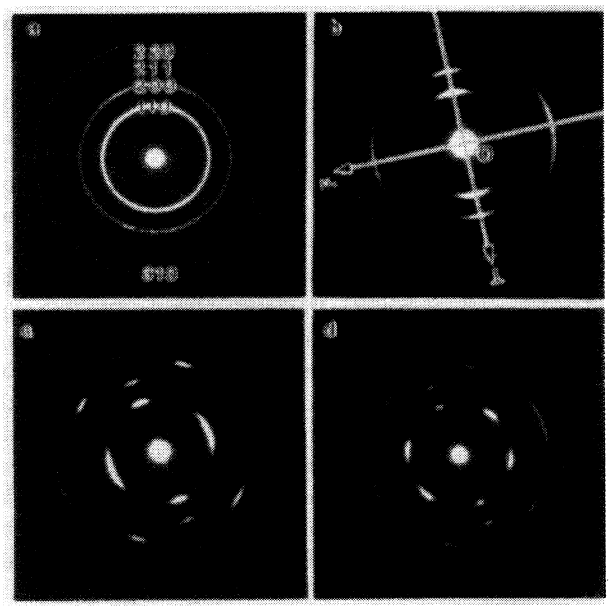

Fig. 9. Electron diffraction patterns of a [001] textured Cr film at (a) 0°, (b) 21°, (c) 45° and (d) 55° tilt.

planes have two distinct angles (90° and 45°) with the [001] direction. The distribution angle α of the [001] textured axis deduced from the slopes of the best fitted straight lines of the $\sin(\omega_0/2)$ vs. $1/\sin(\beta)$ (Fig. 10) and $\cos(\omega_{110}/2)$ vs. $1/\sin(\beta)$ (Fig. 11) plots are 7.1° and 7.9°, respectively.

This technique thus allows us to obtain quantitative information about the crystallographic texture of thin films. It can also be used in multilayer films and the specific orientation relationships can be ascertained from careful examination of a series of tilted electron diffraction patterns.

Conclusions

We have presented some of the methods we have used to improve the properties of magnetic films for recording. These

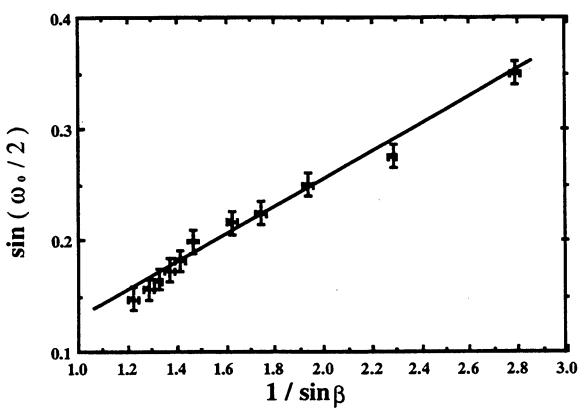

Fig. 10. $\sin(\omega_0/2)$ vs. $1/\sin\beta$ plot of the [001] textured Cr film.

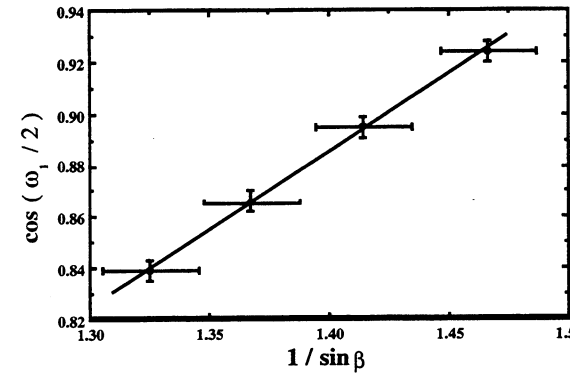

Fig. 11. $\cos(\omega_1/2)$ vs. $1/\sin\beta$ plot of the [001] textured Cr film.

included the use of new underlayer materials, the introduction of intermediate layers between the magnetic film and the underlayer as well as the use of seed layers to control the crystallographic texture of the underlayer. Each of these methods has as its main function the control of one or more of the microstructural features of the magnetic layer. We also presented an overview of our method of studying the crystallographic texture of thin films by electron diffraction and showed one example in the determination of the texture of a Cr thin film underlayer.

Acknowledgments

The work presented in this review has been sponsored in part by the Department of Energy (DE-FG02-90ER45423), the National Science Foundation (ECD 89-07068) and ARPA (MDA97293-1-009). The government has certain rights to this material.

References

[1] J. D. Daval and D. Randet, "Electron microscopy on high-coercive-force Co-Cr composite films," IEEE Trans. Magn., **MAG-6**, 768-773 (1970).

[2] D. E. Laughlin, Y. C. Feng, L.-L. Lee and B. Wong, "Epitaxy and crystallographic texture of thin films for magnetic recording", in *Polycrystalline Thin Films—Structure, Texture, Properties and Applications*, M. Parker, K. Barnak, J. Floro, R. Sinclair and D.A. Smith, eds. MRS publication, vol. **343**, 327-337 (1994).

[3] D. E. Laughlin, B. Cheong, Y. C. Feng, D. N. Lambeth, L.-L. Lee and B. Wong, "The control of microstructural features of thin films for magnetic recording," *Scripta Metallurgica et Materialia* **33** (10/11), 1525-1536 (1995).

[4] L.-L. Lee, D. E. Laughlin and D. N. Lambeth, "NiAl underlayers for CoCrTa magnetic thin films," *IEEE Trans. Magn.*, **30** (6), 3951-3953 (1994).

[5] P. Harllee and D. N. Lambeth, unpublished research.

[6] L.-L. Lee, unpublished research.

[7] L. Fang and D. N. Lambeth, "New high coercivity cobalt alloy thin film medium structure for longitudinal recording," *Appl. Phys. Lett.*, **65** (24), 3137-3139 (1994).

[8] A. Nakamura and M. Futamoto, "Epitaxial growth of Co/Cr bilayer films on MgO single crystal substrates," *Jpn. J. Appl. Phys.*, **32**, (10A), L1410-1413 (1993).

[9] L.-L. Lee, B.K. Cheong, D. E. Laughlin and D. N. Lambeth, "MgO seed layers for CoCrPt/Cr longitudinal magnetic recording media," *Appl. Phys. Lett.*, **67** (24), 3638-3640 (1995).

[10] P. W. Tasker, "Surfaces of magnesia and alumina," *Adv. Ceram.*, **10**, 176-189 (1984).

[11] L. Tang, L.-L. Lee, D. E. Laughlin and D. N. Lambeth, "Study of CoCrPt/NiAl thin films on (001) MgO single crystals", submitted to *Appl. Phys. Lett.*, (1996).

[12] L. Tang and D. E. Laughlin, "Electron diffraction patterns of fibrous and lamellar textured polycrystalline thin films: part I: Theory," in press, *J. Appl. Cryst.*, (1996).

[13] L. Tang, Y. C. Feng, L.-L. Lee and D. E. Laughlin, "Electron diffraction patterns of fibrous and lamellar textured polycrystalline thin films: part II: Applications," in press, *J. Appl. Cryst.*, (1996).

[14] B. K. Vainshtein, "Structure Analysis by Electron Diffraction," p.70, New York: Pergamon, (1964).

[15] P. B. Hirch, A. Howie, R. B. Nicholson, D. W. Pashley and M. J. Whelan, " Electron Microscopy of Thin Crystals," p.116, 2nd ed., Malabar, Florida, Roberte E. Krieger Publishing Company (1978).